Supporting Information

Effect of Salt Selection and Molar Ratio in Molten Salt Synthesis of Single-Crystalline LiNiO$_2$

Wessel van den Bergh,*[a] Rui Yao,[a] Ruizhuo Zhang,[a] Aleksandr Kondrakov,[a,b] Jürgen Janek[a,c] and Torsten Brezesinski*[a]

[a]Battery and Electrochemistry Laboratory (BELLA), Institute of Nanotechnology, Karlsruhe Institute of Technology (KIT), Herrmann-von-Helmholtz-Platz 1, 76344 Eggenstein-Leopoldshafen, Germany
[b]BASF SE, Carl-Bosch-Str. 38, 67056 Ludwigshafen, Germany
[c]Institute of Physical Chemistry & Center for Materials Research (ZfM/LaMa), Justus-Liebig-University Giessen, Heinrich-Buff-Ring 17, 35392 Giessen, Germany

*Email: wessel.j.vdb@gmail.com, torsten.brezesinski@kit.edu

Experimental Methods

Sample Preparation: LNO was prepared from a $Ni(OH)_2$ precursor (d_{50} = 4 µm, BASF SE) and $LiOH \cdot H_2O$ (d_{50} = 4 µm, BASF SE) with salts of varying proportions and molar ratios (see **Table S1**), with the salts being CsCl (Merck KGaA, ≥99.5%), KCl (Merck KGaA, ≥99.5%), K_2SO_4 (Merck KGaA, ≥99.0%), NaCl (Merck KGaA, 99.99%), and Na_2SO_4 (Merck KGaA, ≥98.5%). All samples were dried at 110 °C for >10 h before being stored in an Ar glovebox. Reagents consisting of 1.70 g of $Ni(OH)_2$ and 0.846 g $LiOH \cdot H_2O$ (1.0:1.1 mol. ratio of Ni:Li) along with the chosen salts (1 or 4 mol. eq. to Ni) were mixed via mortar and pestle inside an Ar glovebox until a uniformly light green colored powder was observed (elimination of clumps of white powder, $LiOH \cdot H_2O$). The powder mixture was loaded into an alumina crucible sized either approx. 6 cm × 2.5 cm (half standard) or approx. 9 cm × 2.5 cm (standard) depending on the molar salt ratio used. Powder was evenly distributed and a microspatula was used to cut aeration grooves into the powder to minimize geometric variation in oxidation of precursor. The crucible was loaded into an externally calibrated (see **Figure S41**) tube furnace (Nabertherm, RHTC 80-230/15) equipped with a custom-made quartz glass tube containing a glass line for preheating O_2. Samples were individually calcined at 520 °C for 4 h followed by 880 °C for 12 h with ramping and cooling rates of 5 °C/min and 25 L/h of O_2. Samples were then washed. First, grinding the "frozen block" of material into a powder via mortar and pestle. Next, powder was suspended in 10 mL of DI water for 1-3 min with agitation a total three times (washes), followed by 13 mL of ethanol, then 13 mL of acetone; each wash came with a centrifugation at 3000 rpm for 2 min and a decantation. Once all the washes were completed, the samples were dried with flowing Ar gas to remove majority residual solvent, followed by vacuum drying overnight at room temperature.

SEM Analysis: Samples for SEM were prepared as is after preparation, loaded onto conductive carbon tape and measured on a LEO-1530 (Carl Zeiss AG) at a working distance of approx. 3.5 mm at 10 kV with an In-Lens detector. Sample size was analyzed using ImageJ 1.53t software (National Institute of Health) averaging the Feret diameter of the particle along its longest axis and a second, perpendicular Feret diameter measurement at the midpoint of the first (distance was calibrated via in-image scale bar, see **Figure S1**).

XRD Analysis: Samples were prepared by first sieving through a 90 μm stainless steel mesh to ease packing of a 0.3 mm diameter capillary tube. XRD patterns were collected using a regularly calibrated (LaB$_6$, NIST 660c) STADI P (STOE) diffractometer in Debye-Scherrer geometry with monochromatic Mo K-alpha1 source (λ = 0.7093 Å, 50 kV, 40 mA, polariz. = 0.9528) and a Mythen 1K detector (Dectris). Data were analyzed using GSAS II version 5260 (Argonne National Lab) along a sequential analysis scheme shown below (see **Scheme S1**). Complete set of XRD patterns can be found in **Figures S20**-**S36**, and Rietveld refinement values for all samples prepared are given in **Table S3**.

Electrochemical Testing: The KCl(−) sample after washing and post-annealing at 700 °C for 3 h (with ramping and cooling rates of 5 °C/min and 25 L/h of O$_2$) was electrochemically tested in Li-ion battery (LIB) half-cells (see **Figure S42**). To this end, the material was first mixed with polyvinylidene difluoride binder (PVDF, Solef 5130, Solvay) and Super C65 carbon additive (TIMCAL Ltd.) in N-methyl-pyrrolidone (NMP) in a ratio of 94:3:3 by weight, and then cast onto 0.03 mm thick Al foil using an Erichsen Coatmaster 510 applicator, resulting in an areal loading of ~10 mg/cm^2. We note that all mixing steps were carried out under ambient conditions in a dry room, which can be expected to have some effect on cell performance. The as-prepared cathode tape was dried under vacuum at 120 °C overnight, calendared at 14 N/mm (Sumet Messtechnik), and finally cut into circular 13 mm diameter discs. Coin cells were assembled using a glass fiber GF/D separator, LP57 electrolyte [1 M LiPF$_6$ in a 3:7 by weight of ethylene carbonate (EC) and ethyl methyl carbonate (EMC)], and a Li-metal anode in an Ar glovebox.

Table S1. Complete list of samples prepared with molar ratios of salt to Ni used and fractions of salt used in the mixtures.

Sample ID	Salt Mol. Ratio (X:Ni)	CsCl	KCl	K$_2$SO$_4$	NaCl	Na$_2$SO$_4$
CsCl(−)	1.0	1.0				
CsCl(+)	4.0	1.0				
CsCl-KCl(−)	1.0	0.5	0.5			
CsCl-KCl(+)	4.0	0.5	0.5			
CsCl-NaCl(−)	1.0	0.5			0.5	
CsCl-NaCl(+)	4.0	0.5			0.5	
KCl(−)	1.0		1.0			
KCl(+)	4.0		1.0			

Sample ID						
KCl-K$_2$SO$_4$(−)	1.0		0.75	0.25		
KCl-K$_2$SO$_4$(+)	4.0		0.75	0.25		
KCl-NaCl(−)	1.0		0.5		0.5	
KCl-NaCl(+)	4.0		0.5		0.5	
NaCl(−)	1.0				1.0	
NaCl(+)	4.0				1.0	
NaCl-Na$_2$SO$_4$(−)	1.0				0.54	0.46
NaCl-Na$_2$SO$_4$(+)	4.0				0.54	0.46

Table S2. Complete list of samples prepared with response values.

Sample ID	Avg. Particle size ± stddev. (µm)	d_{10} Particle Size (µm)	d_{50} Particle Size (µm)	d_{90} Particle Size (µm)	Particle Size Span	Ni$_{Li}$ (%)
CsCl(−)	3.33 ± 1.16	1.97035	3.17	4.95795	0.943726	6.93
CsCl(+)	4.00 ± 1.39	2.67585	3.76	6.13645	0.920311	7.56
CsCl-KCl(−)	3.88 ± 1.25	2.492	3.66	5.8725	0.923886	4.98
CsCl-KCl(+)	4.72 ± 1.77	3.1468	4.31	6.8064	0.849292	6.04
CsCl-NaCl(−)	6.17 ± 3.36	2.4681	5.77	10.0892	1.320471	7.24
CsCl-NaCl(+)	10.1 ± 2.81	6.56425	9.96	13.66795	0.713205	6.10
KCl(−)	3.78 ± 1.27	2.504	3.53	5.255	0.779651	4.80
KCl(+)	5.89 ± 2.27	3.5376	5.29	9.00225	1.032332	5.71
KCl-K$_2$SO$_4$(−)	5.14 ± 1.61	3.52575	4.79	7.42155	0.814127	7.08
KCl-K$_2$SO$_4$(+)	8.18 ± 3.48	4.6895	7.69	12.6207	1.031835	7.43
KCl-NaCl(−)	5.04 ± 2.59	2.847	4.04	8.3495	1.362848	5.47
KCl-NaCl(+)	9.01 ± 2.91	5.514	8.63	13.0186	0.869544	7.40
NaCl(−)	11.7 ± 3.51	7.63725	11.4	16.7028	0.79741	5.66
NaCl(+)	14.2 ± 4.11	9.16965	13.4	20.82415	0.870275	5.44
NaCl-Na$_2$SO$_4$(−)	7.75 ± 4.33	3.2711	6.72	14.2407	1.632867	7.12
NaCl-Na$_2$SO$_4$(+)	4.55 ± 1.63	2.77325	4.09	6.57575	0.929025	16.2
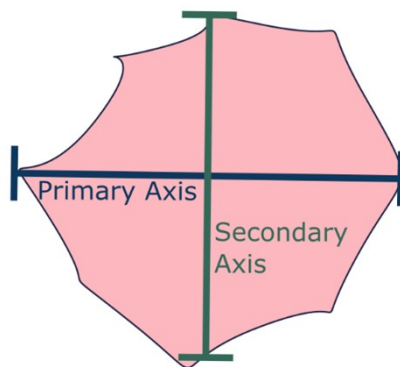
Figure S1. A representation of how particles are measured for size, as described in the SEM section of the Experimental.
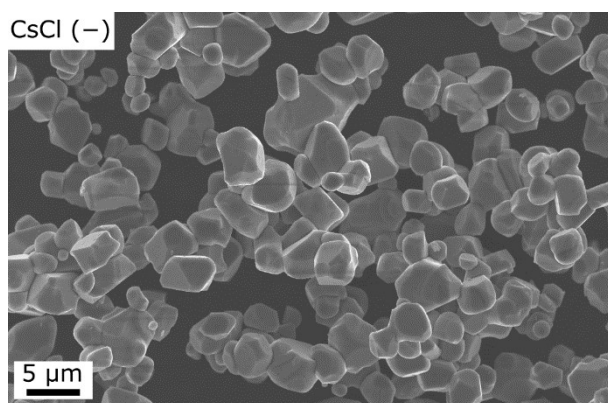
Figure S2. SEM of CsCl(−) sample.
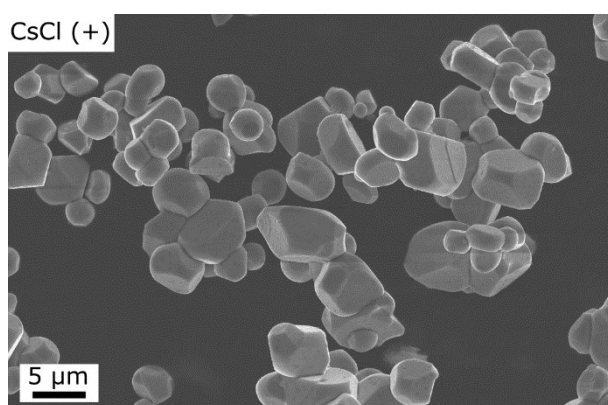
Figure S3. SEM of CsCl(+) sample.
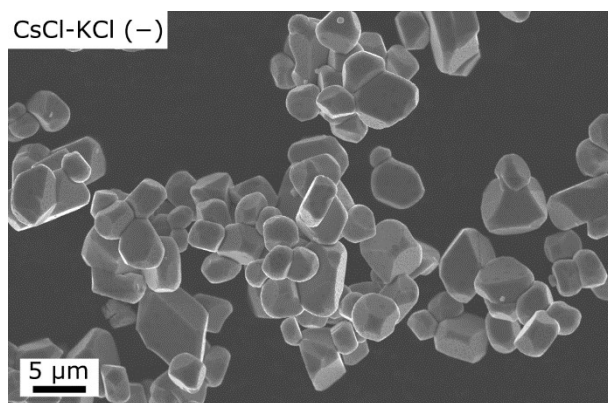
Figure S4. SEM of CsCl-KCl(−) sample.
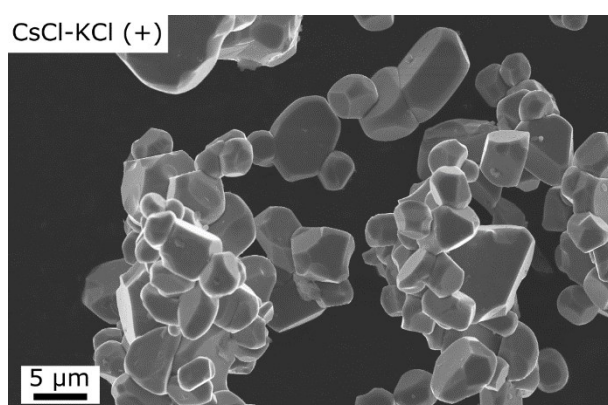
Figure S5. SEM of CsCl-KCl(+) sample.
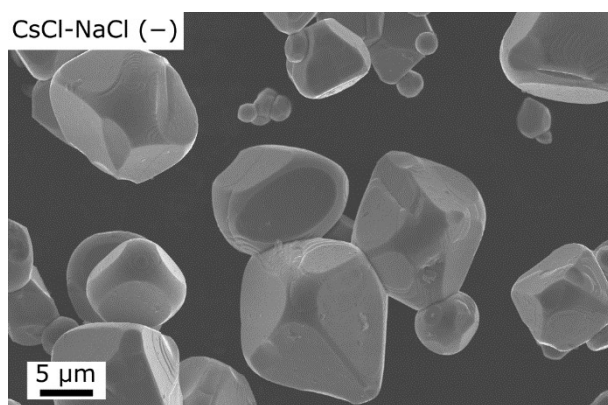
Figure S6. SEM of CsCl-NaCl(−) sample.
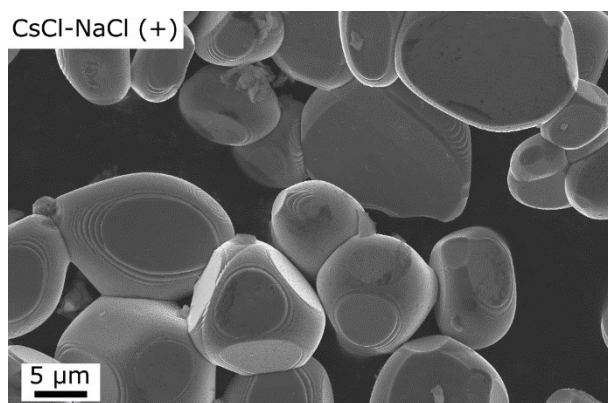
Figure S7. SEM of CsCl-NaCl(+) sample.
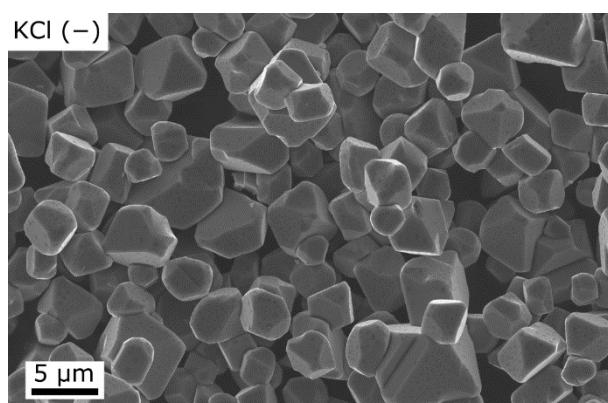
Figure S8. SEM of KCl(−) sample.
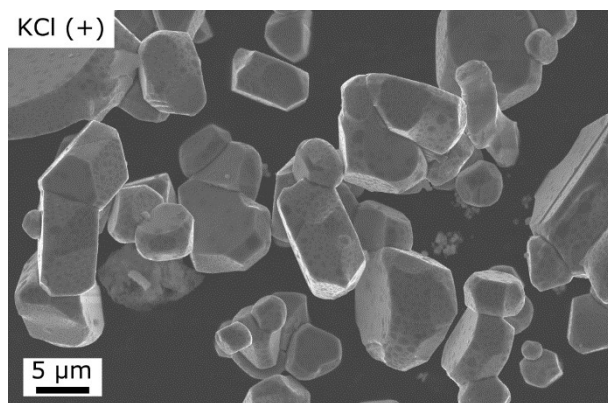
Figure S9. SEM of KCl(+) sample.
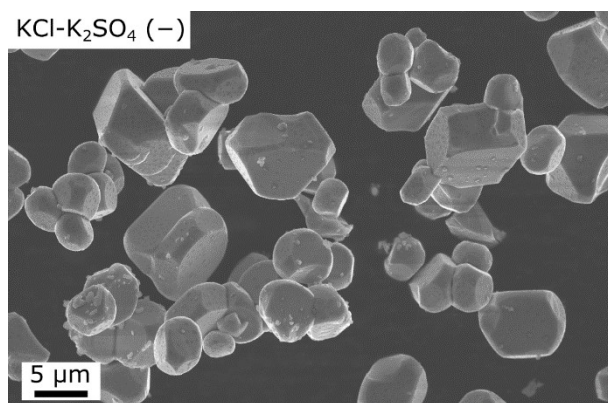
Figure S10. SEM of KCl-K$_2$SO$_4$(−) sample.
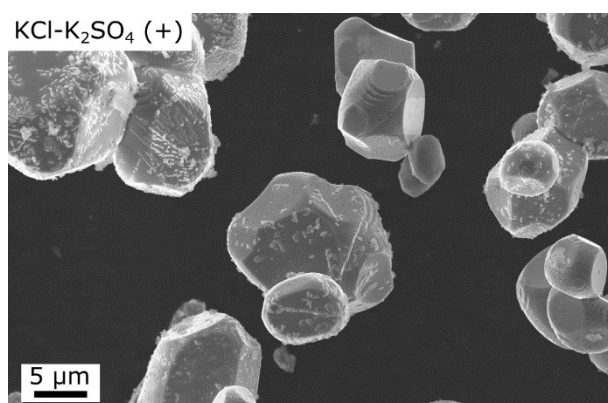
Figure S11. SEM of KCl-K$_2$SO$_4$(+) sample.
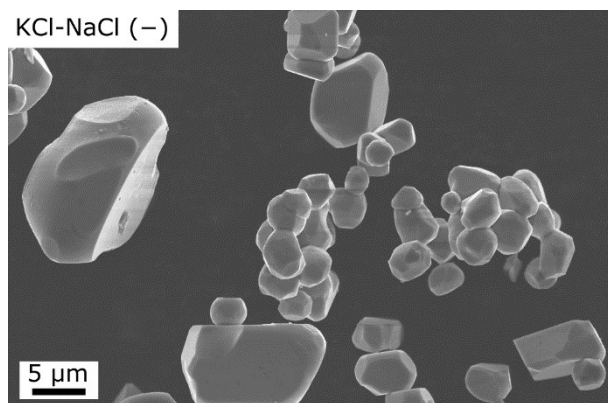
Figure S12. SEM of KCl-NaCl(−) sample.
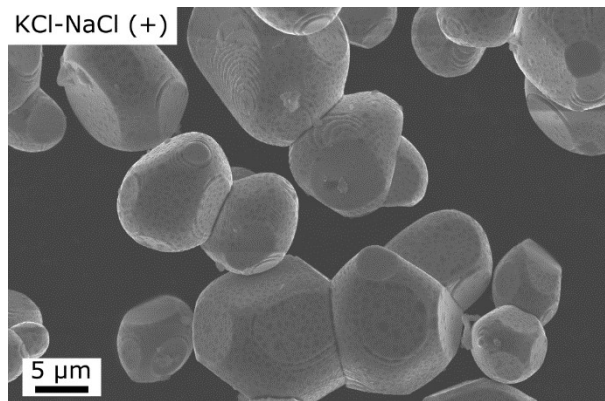
Figure S13. SEM of KCl-NaCl(+) sample.
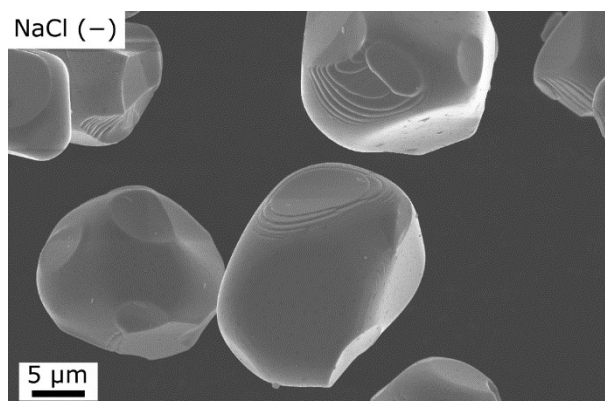
Figure S14. SEM of NaCl(−) sample.
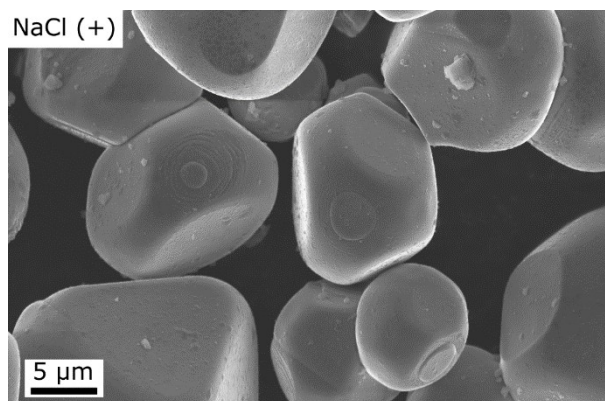
Figure S15. SEM of NaCl(+) sample.
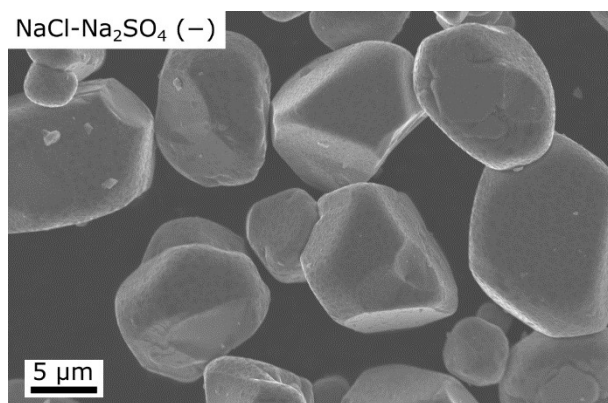
Figure S16. SEM of NaCl-Na$_2$SO$_4$(−) sample.
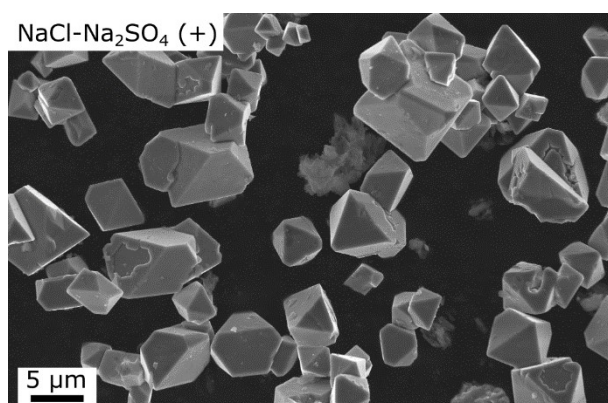
Figure S17. SEM of NaCl-Na$_2$SO$_4$(+) sample.
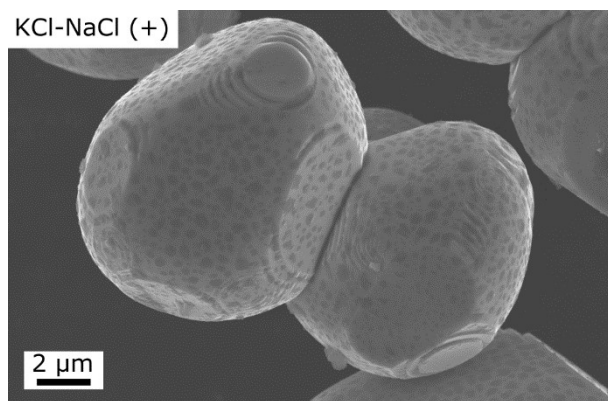
Figure S18. SEM of KCl-NaCl(+) sample with a zoomed in examination of the terracing found on the particles.
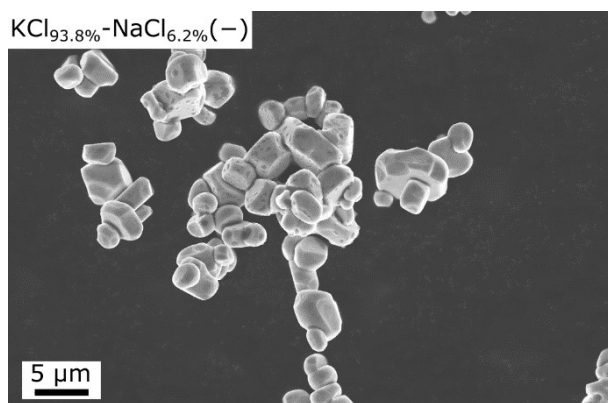
Figure S19. SEM of a tailor-made sample with 93.8% KCl and 6.2% NaCl at 1.0 mol. eq. to Ni.
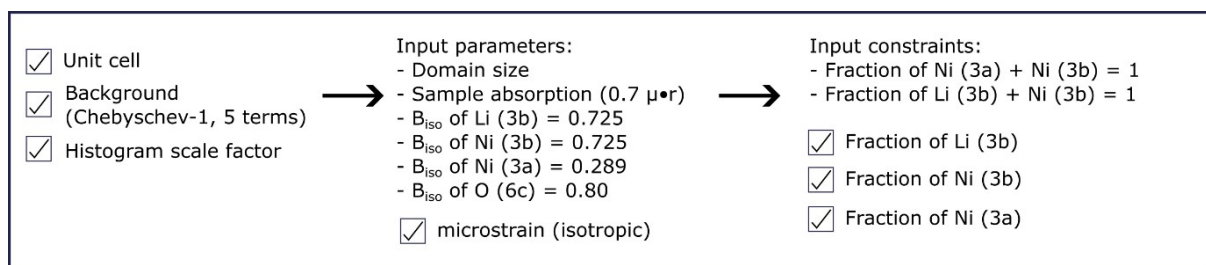
Scheme S1. The sequence of Rietveld refinement performed with GSAS II. Each checked parameter was enabled through further refinements. Input parameters and constraints were held constant.

Table S3. Rietveld refinement values for all samples prepared.

Sample ID	R_{wp} (%)	GoF	a (Å)	c (Å)	V (Å³)	Microstrain	Ni_{Li} (%)
CsCl(−)	19.05	1.19	2.88	14.21	102.42	1362.00	6.93
CsCl(+)	19.35	1.20	2.88	14.21	102.40	448.80	7.56
CsCl-KCl(−)	22.40	1.31	2.88	14.21	102.37	565.20	4.98
CsCl-KCl(+)	19.36	1.20	2.89	14.21	102.44	444.70	6.04
CsCl-NaCl(−)	25.50	1.33	2.89	14.22	102.71	742.70	7.24
CsCl-NaCl(+)	21.49	1.31	2.89	14.21	102.54	469.50	6.10
KCl(−)	22.09	1.17	2.88	14.21	102.33	1322.20	4.80
KCl(+)	20.31	1.28	2.89	14.21	102.44	344.30	5.71
KCl-K₂SO₄(−)	20.81	1.31	2.89	14.21	102.46	469.50	7.08

KCl-K$_2$SO$_4$(+)	20.17	1.25	2.89	14.21	102.49	364.70	7.43
KCl-NaCl($-$)	21.64	1.19	2.88	14.21	102.41	411.30	5.47
KCl-NaCl(+)	19.54	1.22	2.89	14.22	102.53	334.30	7.40
NaCl($-$)	19.87	1.15	2.88	14.21	102.44	77.50	5.66
NaCl(+)	23.15	1.19	2.89	14.22	102.54	1104.50	5.44
NaCl-Na$_2$SO$_4$($-$)	19.44	1.11	2.89	14.22	102.59	696.20	7.12
NaCl-Na$_2$SO$_4$(+)	26.29	1.52	2.90	14.24	103.42	2378.00	16.2
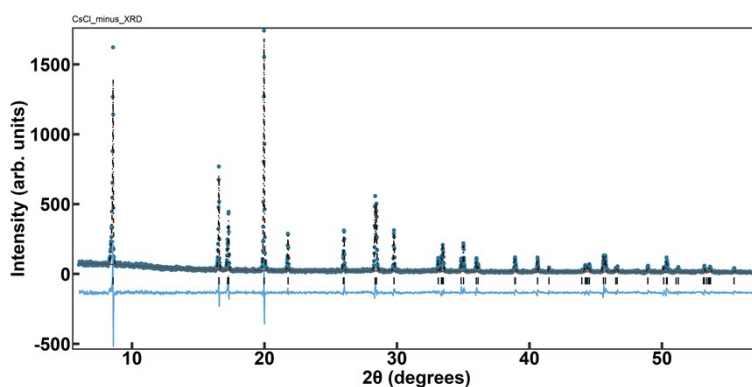
Figure S20. Rietveld refined XRD pattern of CsCl($-$) sample.
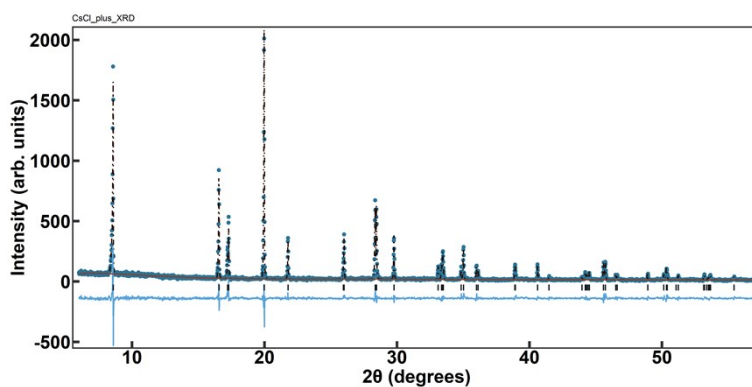
Figure S21. Rietveld refined XRD pattern of CsCl(+) sample.
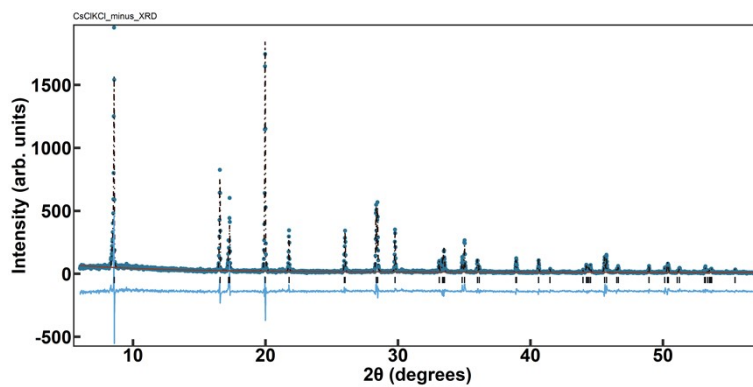
Figure S22. Rietveld refined XRD pattern of CsCl-KCl(−) sample.
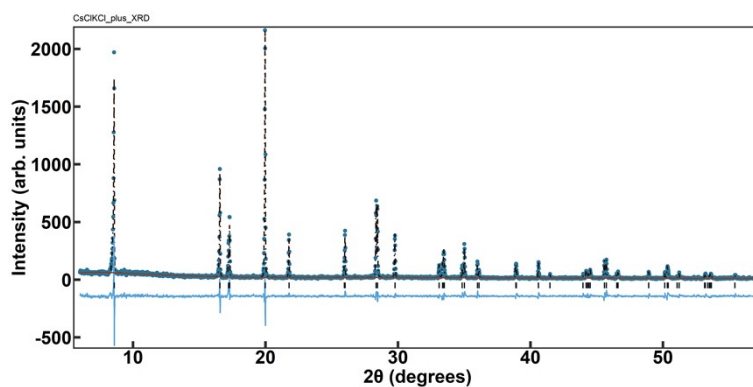
Figure S23. Rietveld refined XRD pattern of CsCl-KCl(+) sample.
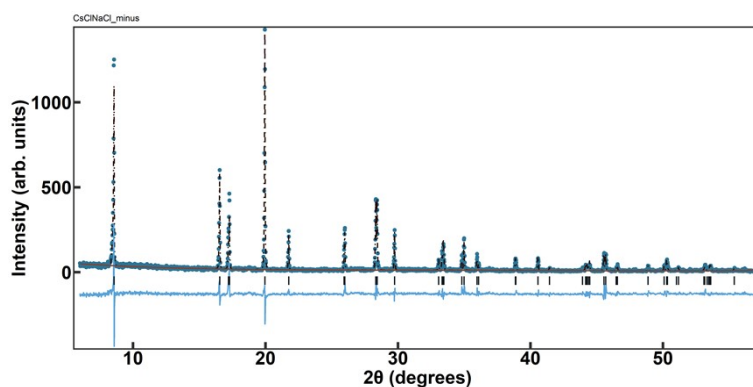
Figure S24. Rietveld refined XRD pattern of CsCl-NaCl(−) sample.
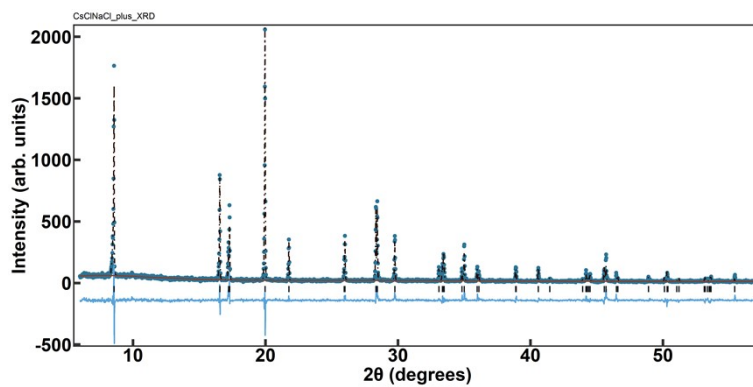
Figure S25. Rietveld refined XRD pattern of CsCl-NaCl(+) sample.
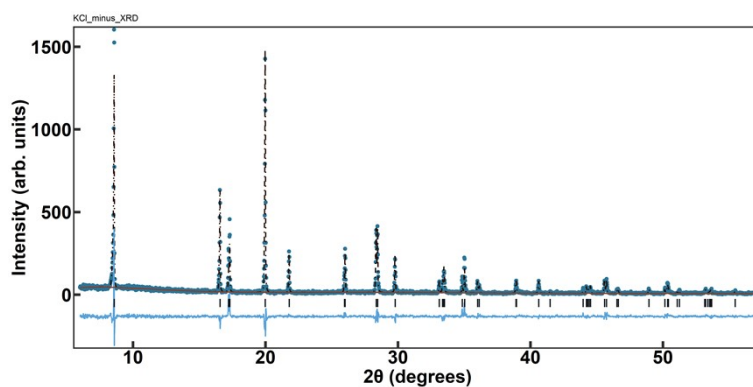
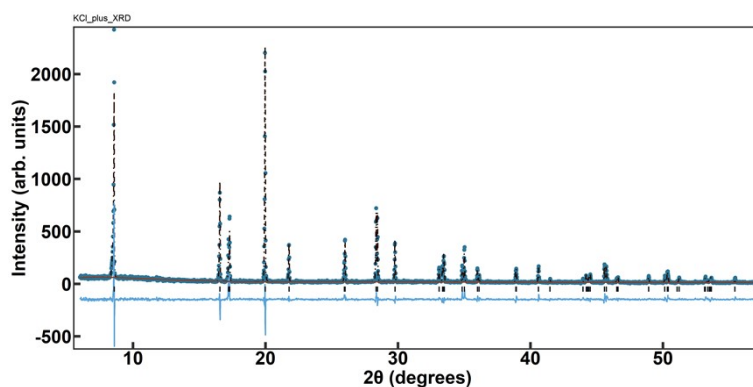**Figure S26.** Rietveld refined XRD pattern of KCl(−) sample.

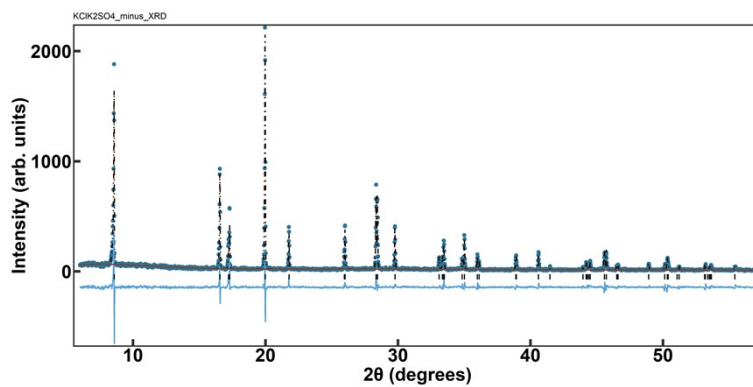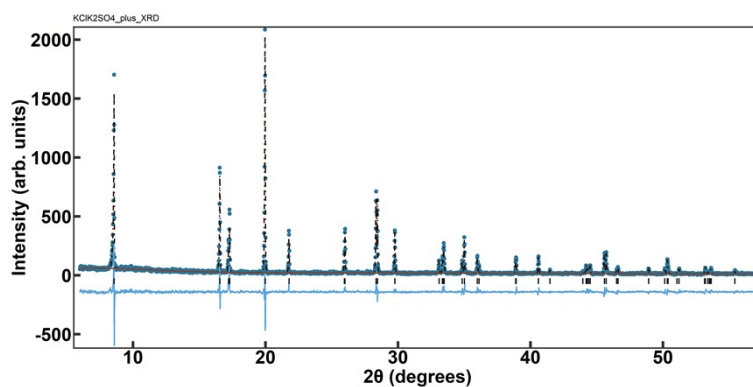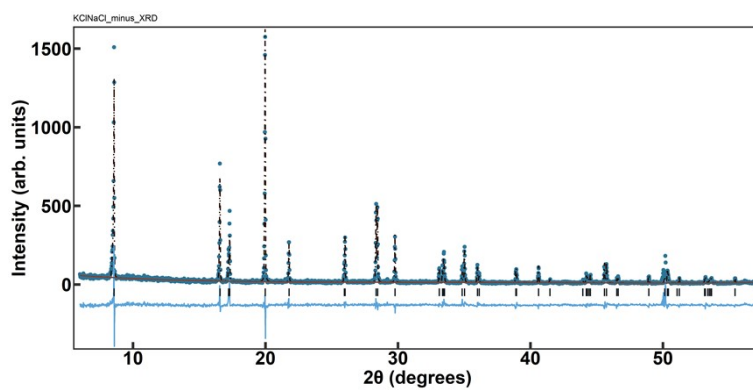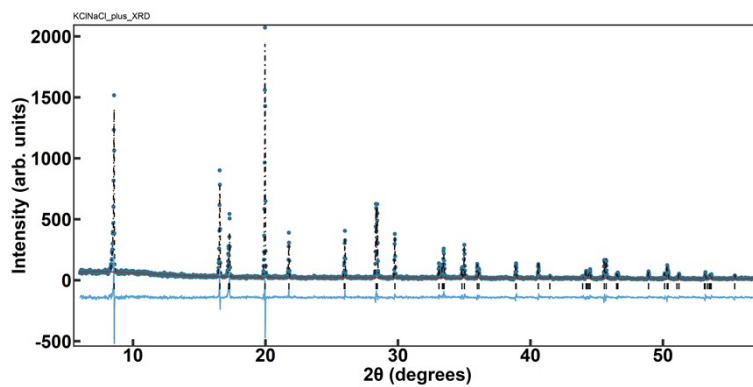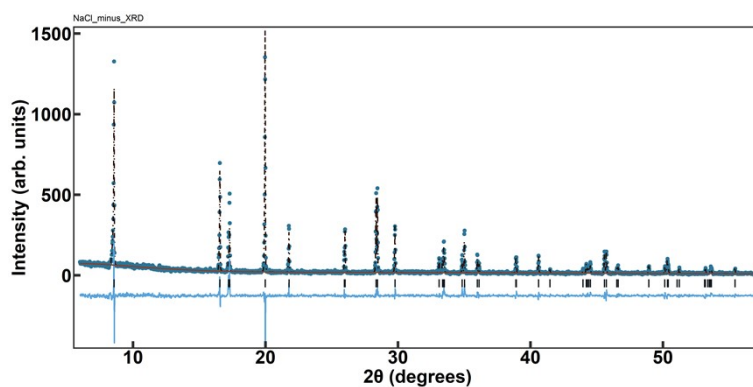**Figure S27.** Rietveld refined XRD pattern of KCl(+) sample.

Figure S28. Rietveld refined XRD pattern of KCl-K$_2$SO$_4$(−) sample.

Figure S29. Rietveld refined XRD pattern of KCl-K$_2$SO$_4$(+) sample.

Figure S30. Rietveld refined XRD pattern of KCl-NaCl(−) sample.

Figure S31. Rietveld refined XRD pattern of KCl-NaCl(+) sample.

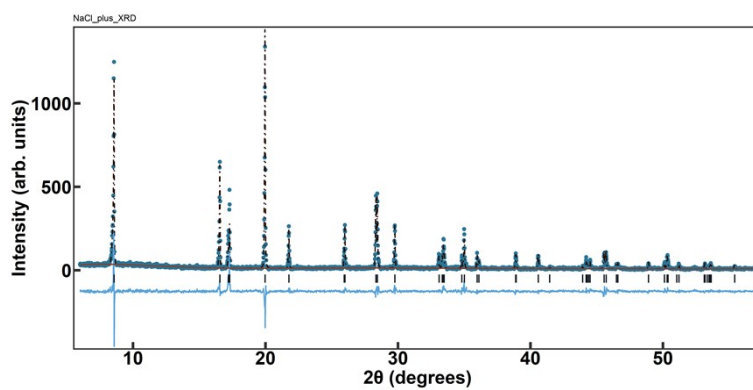**Figure S32.** Rietveld refined XRD pattern of NaCl(−) sample.

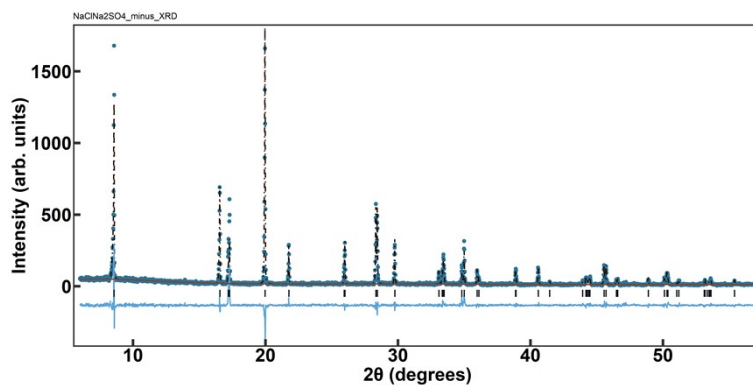**Figure S33.** Rietveld refined XRD pattern of NaCl(+) sample.

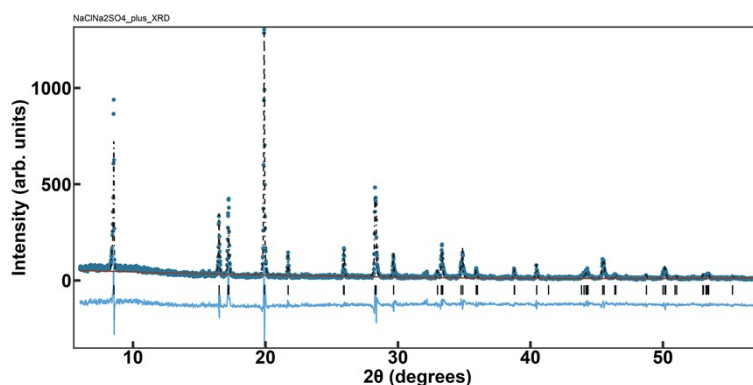**Figure S34.** Rietveld refined XRD pattern of NaCl-Na$_2$SO$_4$(−) sample.

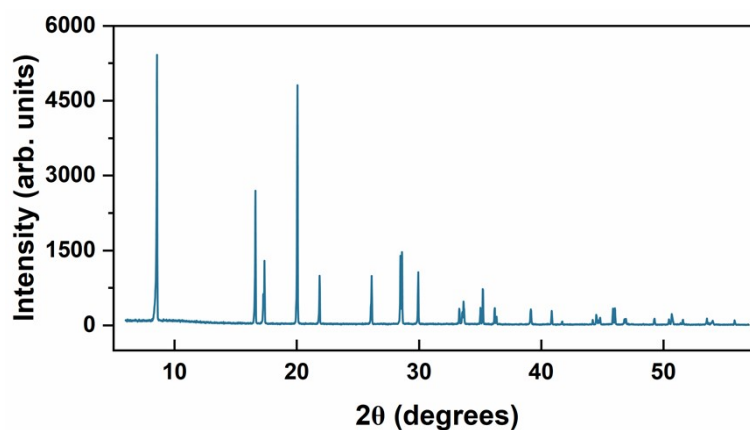**Figure S35.** Rietveld refined XRD pattern of NaCl-Na$_2$SO$_4$(+) sample.

Figure S36. XRD pattern of tailor-made sample with 93.8% KCl and 6.2% NaCl at 1.0 mol. eq. to Ni.

Equation used to calculate particle size span, as shown in **Table S2** and **Figure S37**:

$$Span = \frac{d_{90} - d_{10}}{d_{50}},$$ **Eqn. S1**

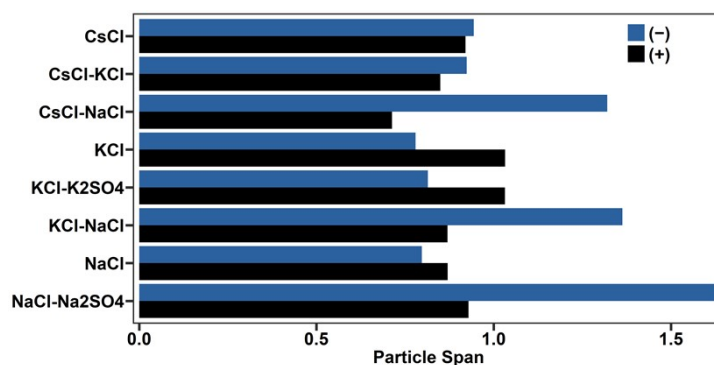where d_i refers to particle sizes at different percentiles of the population.

Figure S37. Bar plot of particle size span for all samples prepared.

Table S4. Estimates of particle span for statistically significant factors accompanied by their standard error and *t*-values.

Term	Estimate	Std. Error	*t*-Ratio	Prob > |*t*|
NaCl[1]	0.93422	0.13546	6.85	>0.0001
KCl[1]	1.0751	0.11592	9.27	>0.0001
CsCl[1]	0.92092	0.13545	6.75	>0.0001
NaCl × Na$_2$SO$_4$	4.5426	0.97734	4.65	0.0007

[1]Due to the nature of a mixture design, the contribution of these factors is convolved with other main effect mixture factors.

Following equations are based upon the estimates of particle span found in **Table S2**:

$$Span = \beta_{NaCl}f_{NaCl} + \beta_{KCl}f_{KCl} + \beta_{CsCl}f_{CsCl} + \beta_{\{NaCl \times Na_2SO_4\}}f_{NaCl}f_{Na_2SO_4}; \quad 1 = \sum_{i=1}^{k}f_i \qquad \textbf{Eqn. S2}$$

and

$$Span = \beta_{NaCl}f_{NaCl} + \beta_{KCl}(1 - f_{NaCl}). \qquad \textbf{Eqn. S3}$$
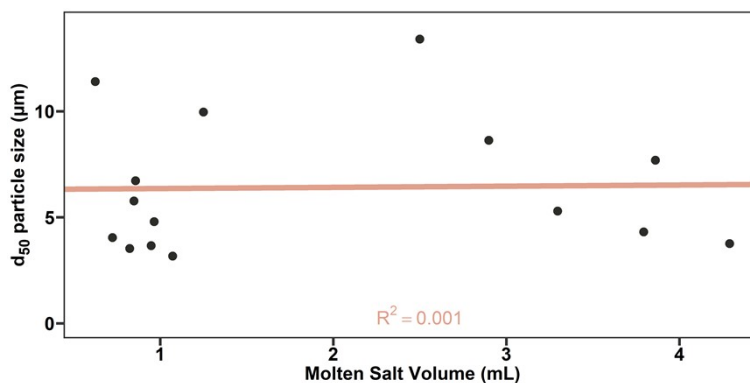
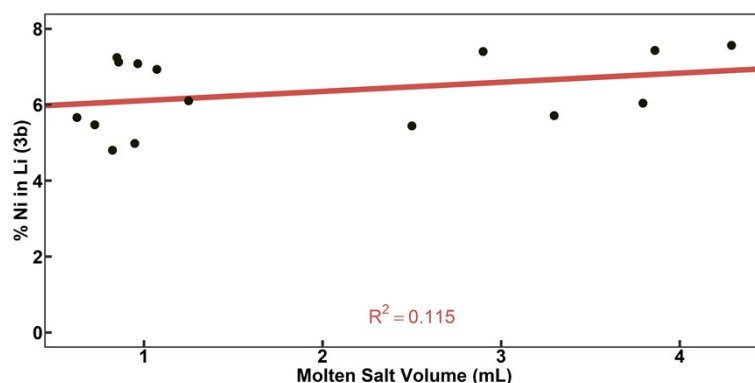**Figure S38.** Linear regression between molten salt volume estimated at 880 °C and d_{50} particle size.

Figure S39. Linear regression between molten salt volume estimated at 880 °C and $Ni^{\bullet}_{Li}$ defect content.
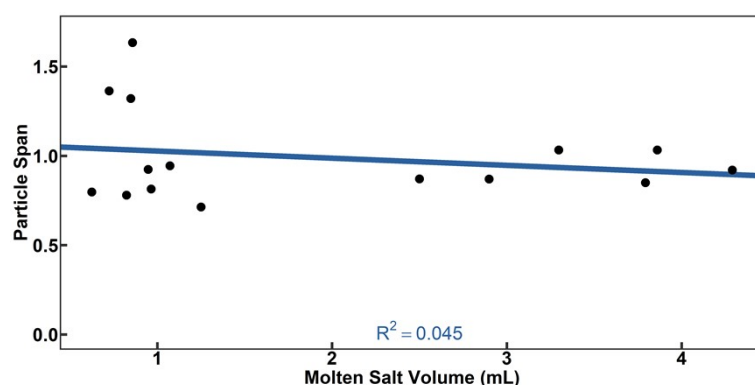

Figure S40. Linear regression between molten salt volume estimated at 880 °C and particle size span.
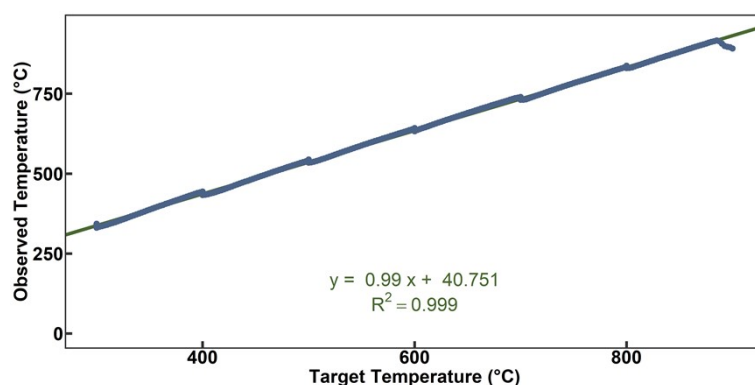

Figure S41. Calibration curve of the furnace used with an OMEGA KHXL-IM60U-RSC-600 thermocouple. Calibration procedure was 30 min holds at 100 °C intervals above 300 °C with 5 °C/min ramps in between each step.
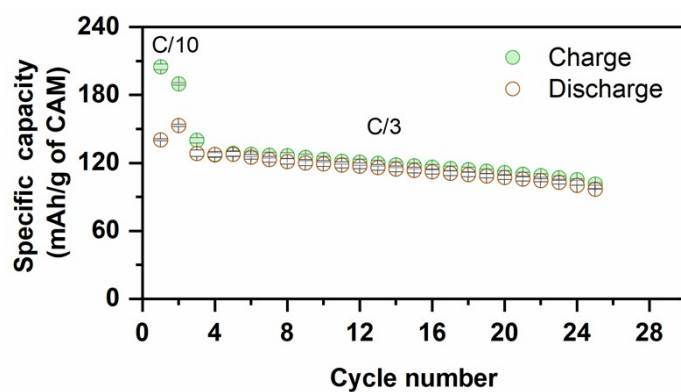
Figure S42. Cycling performance of LIB half-cells using the KCl(−) sample at 25 °C in the potential window of 3.0-4.3 V vs. Li$^+$/Li. The error bars represent the standard deviation from two independent cells.